Photoionization by pulses with a modulated frequency

P. Bała, J. Matulewski, A. Raczyński, and J. Zaremba
Instytut Fizyki, Uniwersytet Mikołaja Kopernika, ulica Grudziądzka 5, 87-100 Toruń, Poland
(Received 10 December 1997)

The dynamics of the bound-state populations and the photoelectron spectra are calculated for model atomic systems irradiated by a pulse with a harmonically modulated frequency. For a system including a single bound state a model is adopted, which takes into account the threshold behavior typical of negative ions and admits continuum-continuum transitions. For a model one-dimensional atom the results are obtained through a numerical integration of the Schrödinger equation. The case of a resonant ionization is also considered. The modulation of the frequency results in changing the instantaneous rate of decay of the initial state, in inducing additional population oscillations for multilevel systems, and in additional peaks in the photoelectron spectra. [S1050-2947(98)01006-3]

PACS number(s): 32.80.Rm, 32.80.Fb, 32.80.Gc

I. INTRODUCTION

This work belongs to a large group of papers devoted to the studies of peculiar aspects of an interaction of atomic systems with a strong laser field. Such studies are still of a vivid interest because one cannot yet say that all the details of the dynamics of such processes are completely understood. An interaction of model atomic systems with laser pulses of various shapes and, in particular, photoionization as its important result have been the subject of numerous papers, in which the dynamics of the decay, i.e., the evolution of populations of the particular states, and the photoelectron spectra are investigated. Exhaustive surveys of the works in this domain have been presented in recent reviews [1–5].

Among the nonperturbative approaches to multiphoton ionization one can distinguish an important class of model studies, in which due to some simplifications one is able to obtain analytical results at least up to some stage of calculations, e.g., essential states' approach, Keldysh-Faisal-Reiss (KFR) methods, or approaches based on approximating the binding potential by contact or separable terms; a complete list of references would be very long and we refer the reader to particular portions of the reviews [1–5]. The present work also belongs to this class.

Recently, in connection with advances in experimental techniques, a growing interest is observed in studying effects of more sophisticated pulses, not only those with a smooth envelope but also two-color [6,7], repeated [8–10], or modulated frequency [11–13] ones. Such situations may be interesting because of the presence of a larger number of controllable parameters. This gives new chances of a more comprehensive external control of the process and in consequence chances of a deeper insight into the details of the dynamics. The technical difficulties in solving the problem theoretically are then essentially increased and one is forced to resort either to a numerical integration of the Schrödinger equation [14–16] (most often for one-dimensional systems, see, e.g., Ref. [17]) or to models including even further simplifications concerning the coupling (see, e.g., Refs. [18–20]).

In Sec. II we propose a model and an approach which enable one to study the effects of short pulses of arbitrary shapes on model atomic systems, with the continuum-continuum transitions taken into account. This is possible due to treating the electron continuum states as free-particle ones and to adopting a special form of the bound-continuum coupling, which, however, reflects salient features of a coupling typical of negative ions. In consequence we are able to perform analytically a large part of the calculations and we are left with an integro-differential equation (in the time variable only) for the nondecay probability amplitude. The structure of this equation is independent of the pulse shape and the same relatively simple computer code can be used to obtain the initial-state decay curves and the photoelectron spectra for any pulses.

The above-mentioned approximation, the essence of which is treating the electron after ionization as a particle free of the influence of the binding potential, is well known in the theory of multiphoton processes; in particular, it constitutes the basis of the Keldysh-Faisal-Reiss approach [5,21]. That approach has been originally formulated to obtain the on-shell S matrix and the photoionization rates in the case of pulses of an infinite duration. The physical consequences of the KFR method have been discussed in numerous papers and, though it seems that there is still no common agreement on its fundamental sense, it is widely used in practical calculations. It is important to stress that the method presented here allows us to obtain the population of the initial state and the bound-continuum transition amplitudes essentially at any time, though long times would require more numerical effort, and also for a significant and quick depopulation of the initial state. Apart from the practical aspect, i.e., the possibility of foreseeing the properties of the initial-state depopulation process and of the photoelectron spectra, our work also has a methodological value, as it formulates a time-dependent approach within the philosophy encountered in the KFR family of methods.

In the final part of Sec. II we describe the pulses with a modulated frequency and we briefly discuss the results of earlier works. Photodetachment by such pulses is a very complicated dynamical process, the studies of which may be important because such pulses can be used to study subtle effects in the neighborhood of resonances or thresholds: one

may control the degree of detuning which varies in time. By changing the depth of the modulation one can regulate the effect of restoring the resonance. This has been demonstrated by Agarwal and Harshawardhan [22,23] for two- and three-level atomic systems. Radmore *et al.* [12] have considered photoionization from a single discrete state to a single structureless continuum (without the lower bound) and have shown that the photoelectron spectra are multipeak, with the heights determined by the values of the Bessel functions, the argument of which is the modulation depth. Raczyński and Zaremba [13] have demonstrated how the results of Radmore *et al.* are modified due to the presence of the threshold. In the present work we show how the previous results are generalized when the threshold is treated properly, continuum-continuum transitions are admitted, and no rotating-wave approximation is made. The results for the dynamics of the decay and the photoelectron spectra, obtained using the methods of Sec. II, are presented and discussed in Sec. III.

In Secs. IV and V we show some model and numerical results for the photoionization of multilevel systems by pulses with a modulated frequency. The results are obtained either by integrating systems of a few differential equations (for atomic systems with a few discrete essential states) or by integrating the one-dimensional time-dependent Schrödinger equation on a grid. In particular, we observe how the presence of the modulation can influence the resonant ionization and the threshold effects.

It is important to stress that, though the adopted parameters which characterize our pulses are now beyond the experimental range, most of our observations concerning the dynamics will remain valid in general. We have chosen such parameters to avoid extensive computations and for demonstrative reasons. Throughout the paper atomic units are used.

II. MODEL PHOTODETACHMENT: THEORY

In this section we present a formalism which enables us to obtain the nondecay probability and the photoelectron spectra for arbitrary pulse shapes, taking into account the existence of the threshold as well as the continuum-continuum transitions.

We consider a model one-electron atomic (ionic) system interacting with a short pulse of a linearly polarized, spatially uniform, classical laser field. The Hamiltonian of the system is

$$H=H_0+V=T+U+V, \quad V=\mathbf{A}\cdot\mathbf{p}+\frac{\mathbf{A}^2}{2}, \tag{1}$$

where T is the kinetic energy, U the binding potential which supports a single bound state $|1\rangle$, and the vector potential $\mathbf{A}$ is given by

$$\mathbf{A}(t)=F(t)\mathbf{e}, \tag{2}$$

$\mathbf{e}=\mathbf{e}_z$ is the polarization, and $F(t)$ is an arbitrary function describing the time dependence of the field.

Our aim is to calculate the amplitudes of the transitions induced by V between the free atomic states $|1\rangle$ and $|\mathbf{k}\rangle$, which satisfy the relations

$$H_0|1\rangle=E_1|1\rangle, \quad H_0|\mathbf{k}\rangle=\epsilon_{\mathbf{k}}|\mathbf{k}\rangle, \tag{3}$$

$$\epsilon_{\mathbf{k}}=\frac{\mathbf{k}^2}{2}.$$

Such a formulation, sometimes called a mixed gauge, is commonly used. Note, however, that it would be more orthodox, though technically more difficult, to look for transition amplitudes between $\exp[-i\mathbf{A}(0)\cdot\mathbf{r}]|1\rangle$ and $\exp[-i\mathbf{A}(t)\cdot\mathbf{r}]|\mathbf{k}\rangle$, which is equivalent to studying transitions between $|1\rangle$ and $|\mathbf{k}\rangle$ induced by the interaction $\mathbf{E}\cdot\mathbf{r}$ in the length gauge [24]. The mixed gauge means asking, e.g., about the transition amplitudes to the states of a given canonical momentum, which in the velocity gauge is different from the kinetic momentum. This means that the energy spectra calculated in this section do not move in an oscillatory manner during the cycle, as would the spectra obtained by projecting onto the states with a given kinetic momentum. In the simplest case of a one-color rectangular pulse the mean kinetic energies differ from the energies $\epsilon_{\mathbf{k}}$ by the value of the ponderomotive shift. If the pulse is switched on and off in a smooth way, i.e., if $\mathbf{A}(t)=\mathbf{0}$ both at the beginning and at the end of the pulse, and its envelope changes slowly compared with the field oscillations, using the mixed gauge yields the exact results for the transition amplitudes after the pulse has been switched off (though not for the time-dependent populations or spectra).

The atomic state vector $|\psi(t)\rangle$ can be written as an expansion

$$|\psi(t)\rangle=\alpha(t)|1\rangle+\int d^3k\beta_{\mathbf{k}}(t)|\mathbf{k}\rangle \tag{4}$$

and the Schrödinger equation leads to the following set of equations for the amplitudes:

$$i\dot{\alpha}=E_1\alpha(t)+\int d^3kF(t)(\mathbf{e}\cdot\mathbf{p})_{1\mathbf{k}}\beta_{\mathbf{k}}(t)+\frac{1}{2}F(t)^2\alpha(t), \tag{5}$$

$$i\dot{\beta}_{\mathbf{k}}=\epsilon_{\mathbf{k}}\beta_{\mathbf{k}}(t)+F(t)(\mathbf{e}\cdot\mathbf{p})_{\mathbf{k}1}\alpha(t)+\frac{1}{2}F(t)^2\beta_{\mathbf{k}}(t)$$

$$+\int d^3k'F(t)(\mathbf{e}\cdot\mathbf{p})_{\mathbf{k}\mathbf{k}'}\beta_{\mathbf{k}'}(t). \tag{6}$$

The initial conditions are $\alpha(0)=1$ and $\beta_{\mathbf{k}}(0)=0$.

We make now the essential approximation in the spirit of a large class of works on atom-strong-field interactions, in particular of the family of Keldysh-Faisal-Reiss approaches [5,21]. In the context of our approach it consists in replacing the continuum U-distorted waves $|\mathbf{k}\rangle$ by the plane waves. The continuum-continuum coupling, present in the last term of Eq. (6), now becomes diagonal in $\mathbf{k}$, i.e., $(\mathbf{e}\cdot\mathbf{p})_{\mathbf{k}\mathbf{k}'}=\mathbf{e}\cdot\mathbf{k}\,\delta(\mathbf{k}-\mathbf{k}')$.

We introduce the modified amplitudes $a(t)$ and $\gamma_{\mathbf{k}}(t)$ by the relations

$$\alpha(t)=\exp\left[-i\left(E_1t+\int_0^t\frac{1}{2}F(t)^2dt\right)\right]a(t), \tag{7}$$

$$\beta_{\mathbf{k}}(t)=\exp\left[-i\left(\epsilon_{\mathbf{k}}t+\int_0^t\frac{1}{2}F(t)^2dt+\int_0^t F(t)\times(\mathbf{e}\cdot\mathbf{k})dt\right)\right]\gamma_{\mathbf{k}}(t). \tag{8}$$

They satisfy the equations

$$i\dot{a}(t)=\int d^3k(\mathbf{e}\cdot\mathbf{p})_{1\mathbf{k}}F(t)\exp\{-i[\epsilon_{\mathbf{k}}t+\mathbf{e}\cdot\mathbf{k}g(t)-E_1t]\}\gamma_{\mathbf{k}}(t), \tag{9}$$

$$i\dot{\gamma}_{\mathbf{k}}(t)=(\mathbf{e}\cdot\mathbf{p})_{\mathbf{k}1}F(t)\exp\{i[\epsilon_{\mathbf{k}}t+\mathbf{e}\cdot\mathbf{k}g(t)-E_1t]\}a(t), \tag{10}$$

where we have set $g(t)=\int_0^t F(t)dt$.

When we integrate Eq. (10) over t and insert the result into Eq. (9) we obtain an integro-differential equation for the amplitude $a(t)$,

$$\dot{a}(t)=-\int_0^t K(t,t')a(t')dt', \tag{11}$$

with the kernel $K(t,t')$ given by

$$K(t,t')=F(t)F(t')\int d^3k|(\mathbf{e}\cdot\mathbf{p})_{1\mathbf{k}}|^2\times\exp\{-i[\epsilon_{\mathbf{k}}(t-t')+\mathbf{e}\cdot\mathbf{k}G(t,t')-E_1(t-t')]\}, \tag{12}$$

where $G(t,t')=g(t)-g(t')$.

As to the bound-continuum coupling, it is known that for the bound state $|1\rangle$ of angular momentum $l=0$ the matrix element for $k\to0$ behaves like k; thus $|(\mathbf{e}\cdot\mathbf{p})_{1\mathbf{k}}|^2k^2dk/d\epsilon_{\mathbf{k}}\sim k^3\sim\epsilon_{\mathbf{k}}^{3/2}$ (Wigner power law [25]). For large energies the coupling tends to zero, for example, in the case of the hydrogen negative ion $|(\mathbf{e}\cdot\mathbf{r})_{1\mathbf{k}}|^2k^2dk/d\epsilon_{\mathbf{k}}$ vanishes as $\epsilon_{\mathbf{k}}^{-5/2}$ [26], which means that the corresponding square matrix element of $\mathbf{e}\cdot\mathbf{p}$ vanishes as $\epsilon_{\mathbf{k}}^{-1/2}$. In the present work, in order to analytically obtain the integral in Eq. (12) we have assumed an exponential cutoff and taken

$$|(\mathbf{e}\cdot\mathbf{p}_{1\mathbf{k}})|^2=\frac{3}{4\pi}C^2k^2\exp(-\gamma\epsilon_{\mathbf{k}})(\mathbf{e}\cdot\hat{\mathbf{k}})^2. \tag{13}$$

We have taken the values of the parameters $C^2=9.184$ a.u., $\gamma=18.14$ a.u., which yield the position and maximum of the coupling (13) equal to that of the H^- ion with $E_1=-0.027\,57$ a.u., imitated by model with a contact potential [27]. We have checked that in the neighborhood of the coupling maximum, which occurs for $\epsilon_{\mathbf{k}}=0.083$ a.u., our formula reproduces the proper value of the coupling. For smaller energies (of order of 0.01 a.u.) our formula underestimates the coupling two to three times, while we do not reach the range of larger energies for which the exponential model reduces the coupling more rapidly than the power function. Our qualitative results will thus be reliable, perhaps except for the overall shift of the whole spectrum due also to highly nonresonant virtual transitions.

The integral in Eq. (12) can now be calculated,

$$\int d^3k|(\mathbf{e}\cdot\mathbf{p})_{1\mathbf{k}}|^2\exp[-i(\epsilon_{\mathbf{k}}\tau+\mathbf{e}\cdot\mathbf{k}G)]=2\pi\int_0^\infty k^4dk\frac{3C^2}{4\pi}\exp\left(-\frac{i}{2}k^2\tau-\frac{1}{2}\gamma k^2\right)\times\int_0^\pi\cos^2\theta\exp(-ikG\cos\theta)\sin\theta d\theta=\frac{3C^2\sqrt{\pi}}{8|G|^5}\left(\rho^{-5/2}-\frac{1}{2}\rho^{-7/2}\right)\exp\left(-\frac{1}{4\rho}\right), \tag{14}$$

where $\tau=t-t'$ and $\rho=(\gamma+i\tau)/2G^2$.

Finally the kernel K has the closed analytical form

$$K(t,t')=3C^2\sqrt{\pi/2}F(t)F(t')e^{iE_1(t-t')}\times\left(\frac{1}{(\gamma+i\tau)^{5/2}}-\frac{G^2}{(\gamma+i\tau)^{7/2}}\right)\exp\left(-\frac{G^2}{2(\gamma+i\tau)}\right). \tag{15}$$

The bound-continuum transition amplitude can be expressed in terms of a single time integral

$$\beta_{\mathbf{k}}=-i\exp\left[-i\left(\epsilon_{\mathbf{k}}t+\frac{1}{2}\int_0^t F(t')^2dt'+\mathbf{e}\cdot\mathbf{k}g(t)\right)\right](\mathbf{e}\cdot\mathbf{p})_{\mathbf{k}1}\times\int_0^t F(t')\exp\{i[\epsilon_{\mathbf{k}}t'+\mathbf{e}\cdot\mathbf{k}g(t')-E_1t']\}a(t')dt'. \tag{16}$$

By the partial wave expansion the ionization amplitude $\beta_{\mathbf{k}}$ can be expressed as a superposition of amplitudes corresponding to transitions to the particular continua numerated by the angular momentum l. Using the formula for the expansion of $\exp(i\mathbf{e}\cdot\mathbf{k}G)$ into $Y_{lm}(\hat{\mathbf{k}})$ and the addition properties of the spherical harmonics we get

$$\beta_{\mathbf{k}}(t)=-i\sqrt{3}Cke^{-\gamma k^2/4}\sum_{l=0}^\infty\beta_lY_{l0}(\hat{\mathbf{k}})\times\exp\left[-i\left(\epsilon_{\mathbf{k}}t+\frac{1}{2}\int_0^t F(t)^2dt\right)\right], \tag{17}$$

with

$$\beta_l=\beta_l(k,t)=\frac{(-i)^{l-1}}{\sqrt{2l+1}}\int_0^t F(t')\exp[i(\epsilon_{\mathbf{k}}t'-E_1t')]\times[lj_{l-1}(kg(t)-kg(t'))-(l+1)j_{l+1}(kg(t)-kg(t'))]a(t'), \tag{18}$$

where j_l are the Bessel functions of half-integer order. The photoelectron energetic spectrum after integrating over angles and including the factors $k^2dk/d\epsilon_k$ stemming from the density of states is given by

$$S(\epsilon_{\mathbf{k}},t)=3C^2k^3\exp\left(-\frac{1}{2}\gamma k^2\right)\sum_l |\beta_l(k,t)|^2. \quad (19)$$

It is understood that the time dependence of the spectrum in Eq. (19) means simply that such a spectrum would be obtained if the pulse $F(t)$ were cut just at the instant t.

The structure of Eq. (18) is quite complicated; note, however, that some general conclusions concerning the qualitative behavior of the amplitudes β can be drawn. If the pulse is rectangular, i.e., $F(t)=(\epsilon_0/\omega)\cos\omega t$, ϵ_0 being the field amplitude, then $g(t)$ is proportional to $\sin\omega t$. If the Bessel functions are expanded into power series in $\sin\omega t'$ and, further, if the amplitude $a(t')$ is assumed to decay exponentially, which is a reasonable approximation in the case of a cw field, then for large t we get β_l as a sum of Lorentz-like terms and the typical above threshold detachment (ATD) spectrum is reproduced [a series of peaks of the same width determined by the imaginary part of the coefficient in the exponent of $a(t)$, separated by the photon energy].

In this paper we concentrate on effects of the pulse frequency modulation, i.e., we take

$$F(t)=\frac{\epsilon_0}{\omega}\cos[\omega t+\xi\sin\omega_1 t], \quad (20)$$

which can in fact be considered as a superposition of pulses of frequencies $\omega,\omega\pm\omega_1,\omega\pm 2\omega_1\ldots$, with the components given by the Bessel functions $J_n(\xi)$ according to the relation

$$\cos(\omega t+\xi\sin\omega_1 t)=\sum_{n=-\infty}^{\infty} J_n(\xi)\cos(\omega+n\omega_1)t. \quad (21)$$

As shown by Agarwal and Harshawardhan [22,23], such a pulse can cause a temporary population trapping in a discrete state at such times at which the instantaneous frequency (see below) does not fit to the resonance between the energy levels. The excitation may be controlled by changing the modulation depth ξ: as follows from Eq. (21), it is, in particular, possible to choose ξ so that $J_m(\xi)=0$ for $\omega\pm m\omega_1$ being the resonant frequency.

Radmore *et al.* [12] have studied photoionization by such a pulse of a simple model system including a single bound state and a single structureless continuum. The usual pole approximation together with the rotating-wave approximation has led them to an exponential decay of the initial-state population. The spectrum is then a sum of Lorentzian terms separated by multiples of ω_1, the amplitudes of which are $J_n(\xi)$; this can be seen from Eq. (16) of this paper, in which $g(t)=0$ and the expansion (21) has been used. By changing the value of ξ Radmore *et al.* could regulate the heights of the peaks, and, in particular, quench symmetrically a pair of the peaks.

In our previous paper [13] we have generalized the results of Radmore *et al.* by admitting the presence of the ionization threshold. We have shown that it is possible to analyze the process again in the spirit of the pole approximation but with an oscillating pole. To briefly present that idea let us, for a moment, make the rotating-wave approximation with respect to the main frequency ω and neglect the continuum-continuum transitions. The kernel $K(t,t')$ of Eq. (12) can then be written as

$$K(t,t')=\frac{\epsilon_0^2}{4\omega^2}\int d^3k|(\mathbf{e}\cdot\mathbf{p})_{1\mathbf{k}}|^2\exp[-i(\epsilon_{\mathbf{k}}-E_1-\omega)(t-t')-\xi(\sin\omega_1 t-\sin\omega_1 t')]. \quad (22)$$

The most important contribution to $K(t,t')$ comes from the region of $t'\approx t$. If we leave only the two lowest terms of the expansion of $\sin\omega_1 t'$ at $t'=t$, we will obtain

$$K(t,t')\approx\frac{\epsilon_0^2}{4\omega^2}\int d^3k|(\mathbf{e}\cdot\mathbf{p})_{1\mathbf{k}}|^2\exp[-i(\epsilon_{\mathbf{k}}-E_1-\omega-\xi\omega_1\cos\omega_1 t)(t-t')]. \quad (23)$$

Therefore it appears useful to introduce the notion of an instantaneous frequency $(d/dt)(\omega t+\xi\sin\omega_1 t)=\omega+\xi\omega_1\cos\omega_1 t$ (see also Refs. [22,23], where the transitions between the discrete states were effective at those time instants in which the instantaneous frequency suited the resonance). It is now possible to repeat the standard steps leading to the pole approximation [8,24], except that here the frequency is time dependent. The instantaneous ionization rate depends on the value of the bound-continuum coupling for the continuum energy reached by the photon with the instantaneous frequency, i.e.,

$$\Gamma=\Gamma(t)=2\pi|V_{1\epsilon}|^2_{|\epsilon=E_1+\omega+\xi\omega_1\cos\omega_1 t}, \quad (24)$$

where $|V_{1\epsilon}|^2=k\epsilon_0^2/(4\omega^2)\int d\hat{k}|(\mathbf{e}\cdot\mathbf{p}_{1\mathbf{k}})|^2$. In particular, $\Gamma(t)=0$ if $E_1+\omega+\xi\omega_1\cos\omega_1 t<0$, while in Ref. [13] we have approximated it by const$\times\epsilon^{1/2}$ above the threshold, in agreement with the Wigner power law [25]. The decay curve for the initial-state population was then composed of pieces of a decreasing curve and of horizontal sections, interchanging twice each modulation period. The spectrum was similar to that of Radmore *et al.*, but Lorentzians were replaced by some higher and narrower lines.

III. MODEL PHOTODETACHMENT: RESULTS AND DISCUSSION

We have performed calculations of the initial-state population and the photoelectron spectra for a few sets of data. We have numerically integrated Eq. (11) for all values of t, then we have calculated the particular spectra (for different l) by performing the integral in Eq. (18) and the total spectrum according to Eq. (19). Below all the decay curves present the nondecay probability as a function of time in atomic units (to obtain time in seconds one has to multiply the abscissas by $2.418\,89\times10^{-17}$). The spectra are probability densities (in atomic units of inverse energy) as functions of energy (in atomic units of energy); to obtain the results in eV the abscissas are to be multiplied and the ordinates divided by 27.2116. The field intensities are in atomic units, the power density in W cm^{-2} is obtained by multiplying ϵ_0^2 by 3.51×10^{16}.

Typical decay curves are shown in Fig. 1 for $\epsilon_0=3\times10^{-3}$ a.u., $\omega=3.2\times10^{-2}$ a.u., $\omega_1=4\times10^{-3}$ a.u., $\xi=2$ (upper curve), $\xi=3.5$ (lower curve). As expected from the crude model considerations of our previous paper [13], we indeed observe flat parts when the instantaneous frequency is

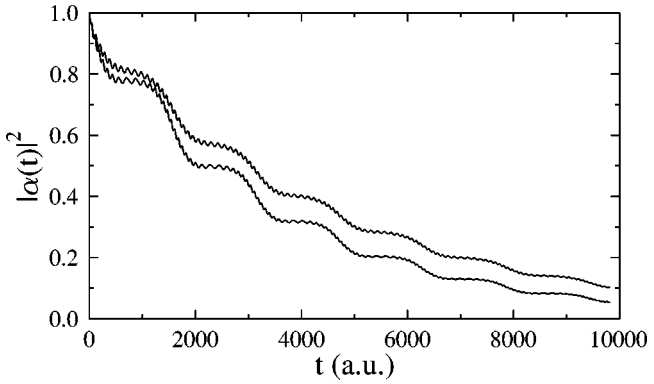

FIG. 1. The population of the initial state for $\epsilon_0=3\times10^{-3}$ a.u., $\omega=3.2\times10^{-2}$ a.u., $\omega_1=4\times10^{-3}$ a.u., $\xi=2$, upper curve; $\xi=3.5$, lower curve.

too small to reach the threshold and steep parts when the detuning above the threshold is maximum — then the bound-continuum coupling is strongest. The flat parts are better visible for the lower curve for which the fraction of the modulation period, in which the laser is effectively tuned below the threshold, is longer. Effectively the decay is quicker in the latter case: the effectiveness of the decay at time intervals of an instantaneous tuning above the threshold increases due to reaching the parts of the continuum the coupling with which is stronger, in spite of an extension of the time intervals in which the detuning is below the threshold.

If the modulation depth is reduced so that $E_1+\omega-\xi\omega_1>0$, i.e., the instantaneous frequency is all the time large enough to ionize, we do not observe quenching of the process, which means that there are no flat parts of the decay curve (apart from the oscillations due to counter-rotating terms of the interaction). We can, however, distinguish the intervals of a quicker and slower decay depending on whether the instantaneous frequency allows reaching parts of the continuum that are more strongly or weakly coupled to the initial state (see Fig. 2, $\epsilon_0=2.5\times10^{-3}$ a.u., $\omega_1=2\times10^{-3}$ a.u., $\xi=1.916$). We have also checked that if the frequency ω is chosen so that $E_1+\omega$ occurs at energy for which the bound-continuum coupling takes maximum, the frequency of the oscillations of the decay curve becomes twice the modulation frequency — the quickest decay occurs now twice in each modulation period, i.e., at those time instants in which the instantaneous frequency allows reaching

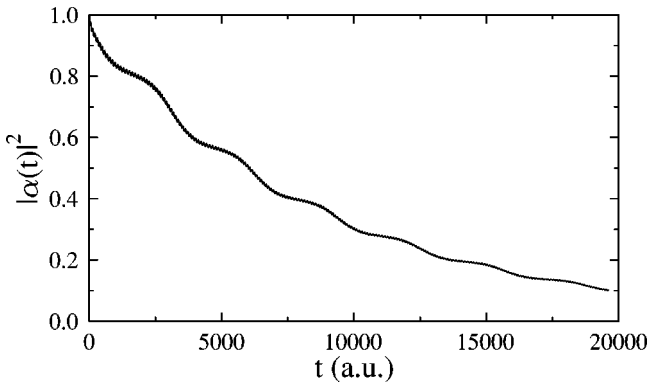

FIG. 2. The population of the initial state for $\epsilon_0=2.5\times10^{-3}$ a.u., $\omega=3.2\times10^{-2}$ a.u., $\omega_1=2\times10^{-3}$ a.u., $\xi=1.916$.

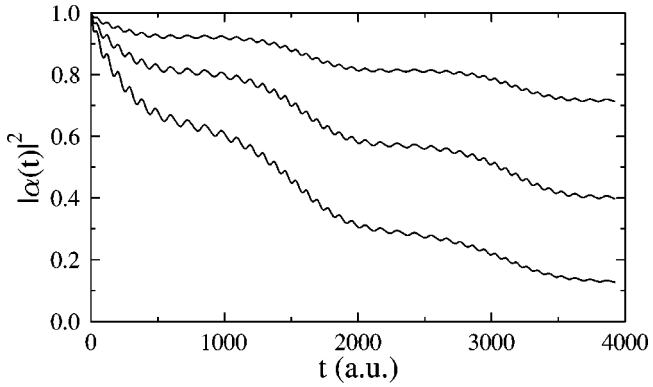

FIG. 3. The population of the initial state for $\epsilon_0=2\times10^{-3}$ a.u., $\omega=3.2\times10^{-2}$ a.u., $\omega_1=4\times10^{-3}$ a.u., $\xi=2$, upper curve; $\epsilon_0=3\times10^{-3}$, middle curve; $\epsilon_0=4\times10^{-3}$, lower curve.

the maximum of the coupling.

The effect of inhibiting the decay due to the instantaneous tuning of the laser below the threshold is reduced for stronger fields when the ionization may occur not solely due to nominally one-photon process. In Fig. 3 we can see how the flat parts of the decay curve for $\epsilon_0=2\times10^{-3}$ a.u., $\omega=3.2\times10^{-2}$ a.u., $\omega_1=4\times10^{-3}$ a.u., $\xi=2$, become leaning for stronger fields of $\epsilon_0=3\times10^{-3}$ a.u. and $\epsilon_0=4\times10^{-3}$ a.u. That this effect is indeed due to continuum-continuum transitions can be seen from Fig. 4 in which the lower curve is again the lower curve of Fig. 3 and the upper curve corresponds to the same field, however, with the continuum-continuum transitions now being neglected.

We should realize that, due to the expansion (21) we have in fact to do with ionization due to a collection of modes with the frequencies $\omega+n\omega_1, n=0,\pm1,\ldots$. The photoelectron spectrum will thus differ from the usual above threshold ionization (ATI) spectrum, which is a set of peaks separated by ω: each peak will be split into subpeaks separated by ω_1, unless the width of the lines becomes of the order of ω_1, when the substructure of the peaks becomes smeared out. In Fig. 5 we can observe the substructures of the first and second ATI peaks for $\epsilon_0=2.5\times10^{-3}$ a.u., $\omega=3.2\times10^{-2}$ a.u., $\omega_1=2\times10^{-3}$ a.u., $\xi=1.916$. For a very strong modulation depth ξ, being of the order of ω/ω_1, the

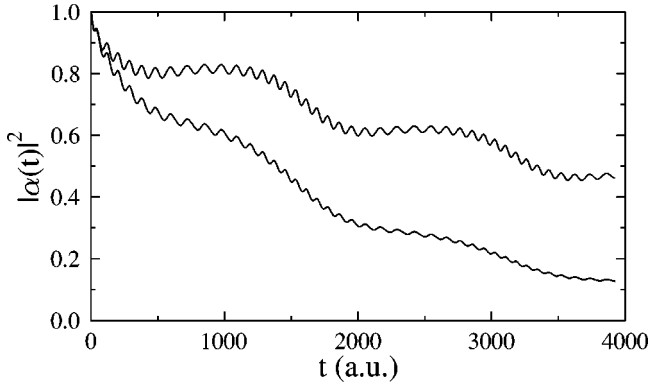

FIG. 4. The population of the initial state for $\epsilon_0=4\times10^{-3}$ a.u., $\omega=3.2\times10^{-2}$ a.u., $\omega_1=4\times10^{-3}$ a.u., $\xi=2$, lower curve; the same but with the continuum-continuum transitions neglected, upper curve.

families of subpeaks due to neighboring peaks may overlap in a coherent way.

The formulas for the spectrum do not allow us to foresee the heights of the subpeaks in the general case. Some conclusions can, however, be drawn in the case of not too strong fields, i.e., when a power expansion with respect to $g(t')$ can be made in the formula (16). Then in the lowest order

$$\beta_{\mathbf{k}}(\infty)^{(1)} = -i\frac{\epsilon_0}{2\omega}(\mathbf{e}\cdot\mathbf{p})_{\mathbf{k}1} \times \int_0^\infty \exp\left[i(\epsilon_{\mathbf{k}} - E_1 - \omega)t - i\xi\sin\omega_1 t - \frac{\Gamma}{2}t\right]dt = \frac{\epsilon_0}{2\omega}(\mathbf{e}\cdot\mathbf{p})_{\mathbf{k}1}\sum_{n=-\infty}^{\infty} J_n(\xi)\frac{1}{\epsilon_{\mathbf{k}} - E_1 - \omega - n\omega_1 + i\Gamma/2}, \tag{25}$$

where we have made the rotating-wave approximation, assumed an exponential decay of the initial state, applied the expansion (21), and skipped the phase factor. The above result implies that the spectrum is a coherent superposition of Lorentzian contributions shifted by multiples of the modulation frequency. A result of this kind has been obtained by Radmore *et al.* [12], who have also stressed that by a special choice of the modulation depth ξ such that $J_m(\xi)=0$ a pair of subpeaks ($\pm m$th) can be removed. In our previous paper [13] we have shown that the Lorentzians are raised and narrowed if, due to oscillations of the instantaneous frequency, ionization is effective only during a part of the modulation period.

The above considerations may be generalized for higher-order terms in $g(t)$, i.e., for the following ATI peaks. For example, the second-order contribution is

$$\beta_{\mathbf{k}}^{(2)}(\infty) = \frac{\epsilon_0^2}{4\omega^2}(\mathbf{e}\cdot\mathbf{p})_{\mathbf{k}1}\mathbf{e}\cdot\mathbf{k}\int_0^\infty dt\exp[i(\epsilon_{\mathbf{k}} - E_1 - \omega)t - i\xi\sin\omega_1 t]\int_0^t dt'\exp[-i\omega t' - i\xi\sin\omega_1 t'] \approx \frac{\epsilon_0^2}{4\omega^2}(\mathbf{e}\cdot\mathbf{p})_{\mathbf{k}1}\mathbf{e}\cdot\mathbf{k}\sum_{n,s=-\infty}^{\infty} J_n(\xi)J_s(\xi)\frac{-1}{(\omega + s\omega_1)} \times \frac{1}{\epsilon_{\mathbf{k}} - E_1 - 2\omega - (n+s)\omega_1 + i\Gamma/2}, \tag{26}$$

where a term, which does not contribute to peaks in the neighborhood of the second ATI peak, has been skipped. The height of the mth subpeak is thus proportional to

$$\sum_{n=-\infty}^{\infty} J_n(\xi)J_{m-n}(\xi)\frac{1}{\omega + (m-n)\omega_1}. \tag{27}$$

The two-photon transition to this part of the continuum, where the mth peak is located, is thus due to an absorption of two photons of frequencies $\omega + n\omega_1$ and $\omega + (m-n)\omega_1$, $m = 0, \pm 1, \pm 2, \ldots$, and the corresponding amplitudes are added in a coherent way.

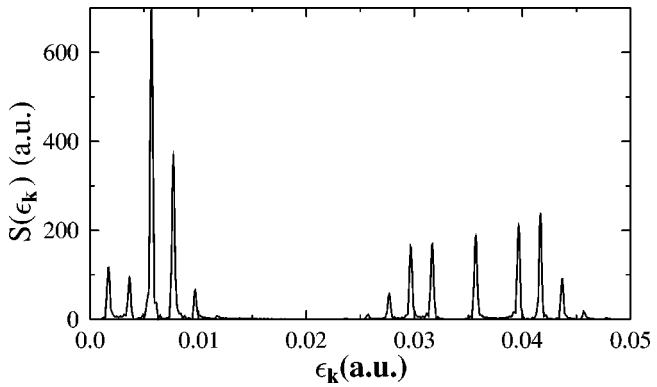

FIG. 5. The substructures of the first and second ATI peaks in the photoelectron spectra for $\epsilon_0 = 2.5\times10^{-3}$ a.u., $\omega = 3.2\times10^{-2}$ a.u., $\omega_1 = 2\times10^{-3}$ a.u., $\xi = 1.916$.

If the modulation frequency ω_1 is much smaller than the fundamental frequency ω, then the above height can be written, due to the identity satisfied by the Bessel functions [28], as

$$\sum_{n=-\infty}^{\infty} J_n(\xi)J_{m-n}(\xi)\frac{1}{\omega} = \frac{1}{\omega}J_m(2\xi). \tag{28}$$

Due to the destructive interference of the amplitudes the mth subpeak of the second ATI peak may be removed by choosing the modulation depth ξ so that $J_m(2\xi)=0$. This approximation is even better than one might expect because the first correction with respect to ω_1/ω then also vanishes [28],

$$\sum_{n=-\infty}^{\infty} J_n(\xi)J_{m-n}(\xi)\frac{(m-n)\omega_1}{\omega} = \frac{\omega_1}{\omega}\frac{m}{2}J_m(2\xi). \tag{29}$$

The modulation depth in the case presented in Fig. 5 was chosen so that $J_1(2\xi)=0$ and indeed the subpeaks numbered 1 and -1 in the second ATI peak are suppressed. The heights of other subpeaks in the figure are approximately equal to those which follow from the above relations.

Note also that a similar argumentation can be repeated *mutatis mutandis* for more-than-two-photon transitions, i.e., for higher ATI peaks. For example, the amplitude of the mth subpeak of the third ATI peak for $\omega_1 \ll \omega$ would be proportional to

$$\sum_{s,j=-\infty}^{\infty} J_s(\xi)J_j(\xi)J_{m-s-j}(\xi) = J_m(3\xi). \tag{30}$$

This result can be further generalized by induction, which means that quenching the mth subpeak in the nth ATI peak requires choosing the modulation depth so that $J_m(n\xi)=0$. From the properties of the Bessel functions it also follows that the number of nonnegligible subpeaks of the nth ATI peak is of the order of the entire part of $2n\xi$.

This analysis of the peaks' heights has been confirmed by our numerical calculations of the spectra; those results are not shown here.

IV. RESONANT IONIZATION OF TWO-LEVEL SYSTEMS

In the process of the resonant ionization of multilevel systems by a pulse with a modulated frequency not only the fact of reaching the continuum but also the resonance conditions can change in time. Consider a simple atomic system including two discrete states $|1\rangle$ and $|2\rangle$ and a single (energy normalized) continuum $|\epsilon\rangle$. It is in principle possible to generalize the approach of Sec. II (in which the continuum-continuum transitions are taken into account) for the systems with two (or more) discrete states. However, since we are here interested mainly in the role of the resonant state, we will limit ourselves to the case of a single continuum; the latter will be coupled only to the upper state.

The probability amplitudes of finding the system in the particular states are, respectively, a, b, and c_ϵ. They satisfy the equations in the interaction picture and in the rotating-wave approximation

$$
\begin{aligned}
i\dot{a} &= \exp[i(E_1-E_2+\omega)t+i\xi\sin\omega_1 t]vb,\\
i\dot{b} &= \exp[i(E_2-E_1-\omega)t-i\xi\ \sin\omega_1 t]va\\
&\quad+\int d\epsilon\exp[i(E_2-\epsilon+\omega)t+i\xi\sin\omega_1 t]V_{2\epsilon}c_\epsilon,\\
i\dot{c}_\epsilon &= \exp[i(\epsilon-E_2-\omega)t-i\xi\sin\omega_1 t]V_{\epsilon 2}b,
\end{aligned}
\tag{31}
$$

where $v=(\epsilon_0/2\omega)(\mathbf{e}\cdot\mathbf{p})_{12}$, and $V_{1\epsilon}=(\epsilon_0/2\omega)(\mathbf{e}\cdot\mathbf{p})_{1\epsilon}$. If again the coupling of the upper state with the continuum is treated in the pole approximation with a moving pole, the second of the above equations becomes

$$
i\dot{b}=\exp[i(E_2-E_1-\omega)t-i\xi\sin\omega_1 t]va-\frac{i\Gamma(t)}{2}b,
\tag{32}
$$

with $\Gamma(t)=2\pi|V_{2\epsilon}|^2_{|\epsilon=E_2+\omega+\xi\omega_1\cos\omega_1 t}$.

As pointed out by Agarwal and Harshawardhan [22,23], who, however, did not discuss ionization, the character and interpretation of the results depend on the relation between the Rabi frequency (equal to v in the resonance conditions) and the modulation frequency ω_1.

If the modulation frequency is large, then at most one component (say jth) of the expansion (21), namely, that for which $|E_2-E_1-\omega-j\omega_1|$ is smallest, is significant for the 1-2 transition. Then we have in fact to do with a two-state damped Rabi system [two atomic states coupled by a monochromatic field of frequency $\omega+j\omega_1$ and of the coupling strength $vJ_j(g)$], only slightly perturbed by the fields of frequencies $\omega+s\omega_1, s\neq j$. In Fig. 6 we show the populations of the two discrete states and the ionization probability as functions of time for $d_1\equiv E_2-E_1-\omega=0.004$ a.u., $\omega_1=0.004$ a.u., $v=0.001$ a.u., $\xi=2.405$ (first zero of J_0), and $\Gamma(t)=0.0002$ a.u.$=$const (the latter means that no threshold effects are present). The distance between the peaks is to a good approximation $\pi/[vJ_1(\xi)]$, as expected, because the resonance is restored by photons with $j=1$. If the value of ξ is chosen so that $J_1(\xi)=0$, the results are drastically changed: both excitation and ionization are suppressed because no photons necessary for the resonant transition are present. In Fig. 7 we show the populations and the ionization probability for $\xi=3.83$ (first zero of J_1).

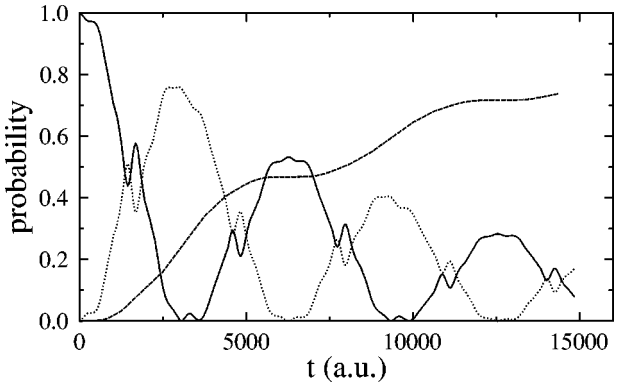

FIG. 6. The populations of the two discrete states (oscillating curves) and the total ionization probability for $d_1=\omega_1=0.004$ a.u., $v=0.001$ a.u., $\xi=2.405$, and $\Gamma(t)=0.0002=$const (no threshold effects). At $t=0$ the population was in the lower state.

When the instantaneous frequency causes crossing the ionization threshold, the results can be further modified: ionization is possible only in those time intervals in which $d_2+g\omega_1\cos\omega_1 t>0$, where $d_2\equiv E_2+\omega$. On the other hand, ionization is more probable in those time intervals in which the population of the upper state is largest. It is possible to combine the parameters so that just in those intervals the instantaneous frequency is too small to allow ionization. To account for the proper threshold behavior we have assumed that the bound-continuum coupling $|V_{2\epsilon}|^2$ in the case of an s continuum is proportional to $\epsilon^{1/2}$ according to the Wigner power law. In consequence $\Gamma(t)=\eta\mathrm{Re}[d_2+\xi\omega_1\cos\omega_1 t]^{1/2}$, η being a constant which gives account of the coupling strength. The results are shown in Fig. 8 and Fig. 9 where we present the population of the upper state and the ionization probability for $v=0.004$ a.u., $d_1=0.004$ a.u., $\omega_1=0.004$ a.u., $\xi=2.405$, $\eta=0.003$ a.u., and additionally $d_2=0.02$ a.u. (no threshold crossing) for Fig. 8 and $d_2=-0.004$ a.u. for Fig. 9. Indeed, ionization is strongly suppressed in the latter case because the transition from the upper state to the continuum is possible just at the moments at which its population is minimum. The sinusoidal character of the Rabi oscillations of the frequency $v|J_{-1}(\xi)|$ is distorted due to the components of the pulse with the frequencies $\omega+n\omega_1$ with $n\neq-1$.

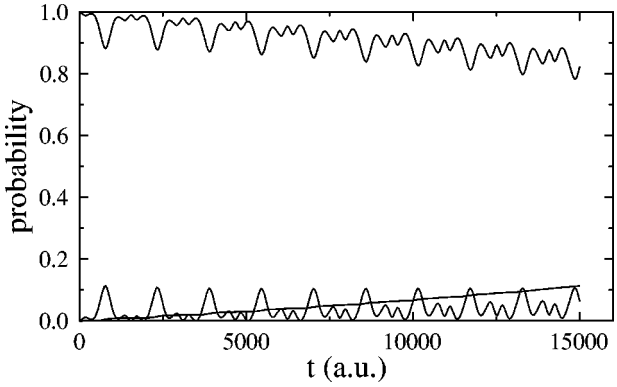

FIG. 7. As in Fig. 6 but for $\xi=3.83$.

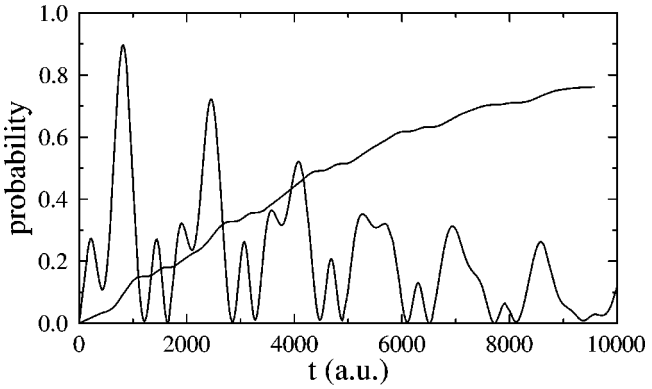

FIG. 8. The population of the upper state (oscillating curve) and the ionization probability with the threshold taken into account for $v=d_1=\omega_1=0.004$ a.u., $d_2=0.02$ a.u., $\xi=2.405$, $\eta=0.003$ a.u.

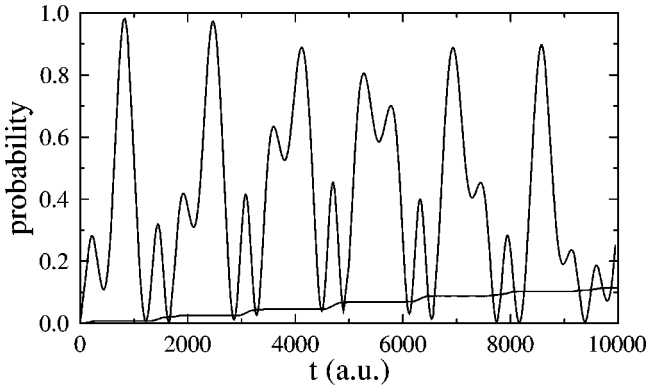

FIG. 9. As in Fig. 8 but for $d_2=-0.004$ a.u.

A quite different picture is observed if the Rabi frequency v is significantly larger than the modulation frequency. Then the transition between the discrete states can be induced by many components of the field of frequencies $\omega+j\omega_1$. The notion of an instantaneous frequency is now useful in the description of the 1-2 transition. For a monochromatic field we would observe fast oscillations of the populations of the states 1 and 2 and the depth of the modulations would depend on how far from resonance the frequency occurs. For a pulse with a modulated frequency the detuning changes in time so the depth of the fast oscillations oscillates itself with the frequency ω_1. The changes in the populations are largest in those time intervals in which we have an instantaneous resonance. This is shown in Fig. 10 where we present the lower state population and the ionization probability for the same data as in Fig. 7 except that $v=0.01$ a.u. Now the qualitative features of the picture do not depend on whether $J_j(\xi)=0$ for any value of j, in contradistinction to what is suggested in the paper of Agarwal and Harshawardhan [22] (in the case of a two-level system).

As to the spectrum, we do not present here any quantitative results, but their qualitative properties follow from the general Floquet theory, which predicts the form of the solutions of the first of Eqs. (31) and Eq. (32). In particular $b(t)$ can be written as

$$b(t)=\exp(-i\lambda_1 t)\sum_{n=-\infty}^{\infty} r_n \exp(in\omega_1 t) + \exp(-i\lambda_2 t)\sum_{n=-\infty}^{\infty} s_n \exp(in\omega_1 t), \tag{33}$$

where $\lambda_{1,2}$ are some complex numbers and r_n and s_n are the expansion coefficients of the periodic functions into Fourier series. After the above solution has been inserted into the third of Eqs. (31) and integrated, we obtain

$$c_\epsilon(\infty)=V_{\epsilon 2}\sum_{j=-\infty}^{\infty} J_j(\xi)\sum_{n=-\infty}^{\infty}\left(\frac{r_n}{\epsilon-E_2-\omega-(j-n)\omega_1-\lambda_1} + \frac{s_n}{\epsilon-E_2-\omega-(j-n)\omega_1-\lambda_2}\right). \tag{34}$$

Clearly $\mathrm{Re}\lambda_{1,2}$ are responsible for the shift and $\mathrm{Im}\lambda_{1,2}$ for the width of the peaks. For a small modulation frequency and a large 1-2 coupling the spectrum has the form of an Autler-Townes (AT) doublet with each of the peaks split into subpeaks separated by the modulation frequency. In the opposite case, i.e., for a large modulation frequency and a small 1-2 coupling, the spectrum is a set of AT doublets separated by the modulation frequency. In the intermediate regime one can expect the interference of the splitting effects due to both frequency modulation and two states.

V. PHOTOIONIZATION OF MULTILEVEL SYSTEMS

Let us now check the effect of pulses with a modulated frequency on a system, the energy spectrum of which resembles that of real atoms. Such a system in the form of a one-dimensional atom has often been used in the discussion of strong-field photoionization [29]. The Hamiltonian reads

$$H=-\frac{1}{2}\frac{\partial^2}{\partial x^2}-\frac{1}{(x^2+1)^{1/2}}+x\epsilon_0\cos(\omega t+\xi\sin\omega_1 t+\phi). \tag{35}$$

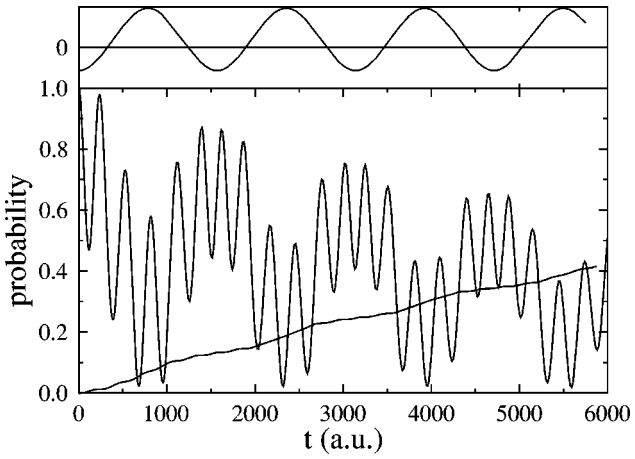

FIG. 10. The population of the lower state (oscillating curve) and the ionization probability for $v=0.01$ a.u. and other parameters as in Fig. 7. Also shown the time-dependent detuning $d_1-\xi\omega_1\cos\omega_1 t$ (in arbitrary units).

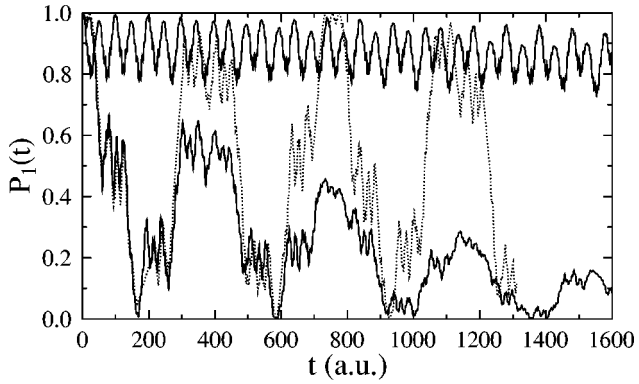

FIG. 11. The population of the initial (ground) state of the one-dimensional atom for $\epsilon_0=0.05$ a.u., $\omega=0.518\,314$ a.u., $\omega_1=0.058\,77$ a.u., $\phi=\frac{3}{2}\pi$, $\xi=0.1$, upper solid curve; $\xi=3.8$, lower solid curve. The dotted curve describes the evolution of this population in the case of the atomic model including only three lowest states.

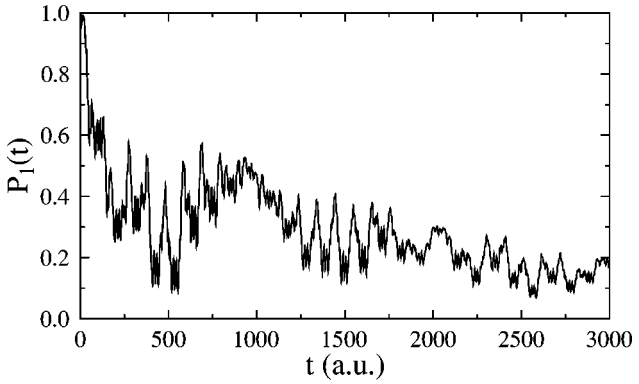

FIG. 12. The population of the initial state of the one-dimensional atom for $\xi=5.13$ and other parameters as in Fig. 11.

Due to its long range character the ''regularized Coulomb'' binding potential supports an infinite number of bound states, of which eigenenergies and eigenvectors are computed numerically, as well as the scattering states. The eigenenergies $E_n, n=1,2,\ldots,$ and the coupling matrix elements x_{jk} can be found in Ref. [29]. It is assumed that initially the atom was in the ground state. The atom-field interaction is now taken in the length gauge. The time-dependent Schrödinger equation has been integrated numerically on a grid, with the time evolution operator expanded into the Chebyshev polynomials. The details of the numerical procedure can be found in Refs. [30,31]. The numerical methods of such a kind are effective for not too long times, because they are very time-consuming. In Fig. 11 we show the time evolution of the initial-state population for $\epsilon_0=0.05$ a.u., $\omega=0.518\,314$ a.u., $\omega_1=0.058\,77$ a.u., $\phi=3\pi/2$. These values of the parameters correspond to the situation in which the frequency ω is equal to the energy interval E_3-E_1, $\omega+\omega_1=E_4-E_1$, and $\omega-2\omega_1\approx E_2-E_1$; the ionization is nominally a two-photon one. The time integration was over 128 optical periods. For $\xi=0.1$ (almost no frequency modulation) we observe small oscillations corresponding to a nonresonant, weakly damped Rabi problem for the states 1 and 2. For $\xi=3.8$ (first zero of J_1) the character is essentially changed. Due to the presence of the photons of frequency $\omega-2\omega_1$ we have to do with a nearly resonant coupling of the states 1 and 2. However, the ''frequency'' of the damped oscillations is not exactly the Rabi frequency of the two-level system. We have checked by solving the two- and three-state problem numerically that including the coupling of state 2 with state 3 essentially improves the agreement of the two frequencies. The rapid oscillations are due to other nonresonant processes, i.e., the coupling of states 1 and 2 by photons of frequencies other than $\omega-2\omega_1$ and also by counter-rotating terms of the Hamiltonian. For this special value of ξ, $J_1(\xi)\approx 0$ so no coupling of the states 1 and 4 is present, but this coupling would not be very important because of a relatively weak dipole coupling of those states.

The picture is very much different for $\xi=5.13$, i.e., when $J_{-2}(\xi)=0$, so photons which could produce a dominating resonant 1-2 coupling are absent (Fig. 12). One cannot identify any dominating frequency close to a particular Rabi frequency. Instead one can observe oscillations corresponding to the modulation frequency ω_1. This is consistent with the observations from the preceding section.

The photoelectron spectra have been obtained by projecting the time-dependent wave function on field-free scattering states (both even and odd). Because the photoelectrons are subject to a jittering motion in the laser field, the spectra are not stationary: they oscillate in the rhythm of the field. Our spectra have been obtained for times equal to a full number of cycles plus such a fraction of a cycle that the instantaneous classical velocity of the electron jittering motion is zero. At those time instants

$$A(t)=-\int_0^t \epsilon_0\cos(\omega t+\xi\sin\omega_1 t+\phi)dt=0, \qquad (36)$$

or, in other words, the kinetic momentum is equal to the canonical momentum. Note that for nonmonochromatic fields the oscillations of the peaks' positions are more complicated than in the case of a purely harmonic field.

In Fig. 13 we show the photoelectron spectrum for a weakly frequency-modulated pulse ($\xi=0.3$) with other parameters as in Fig. 11 and Fig. 12. Because the excitation is far from resonance, the spectrum in the case of a harmonic pulse should reflect the energetic structure of the atom [32]: the three main subpeaks of the first ATI peak, which occur at $E_2+\omega\approx 0.243$ a.u., $E_1+2\omega\approx 0.366$ a.u., and $E_4+\omega\approx 0.425$ a.u., are indeed visible in the case of $\xi=0.3$. Due to

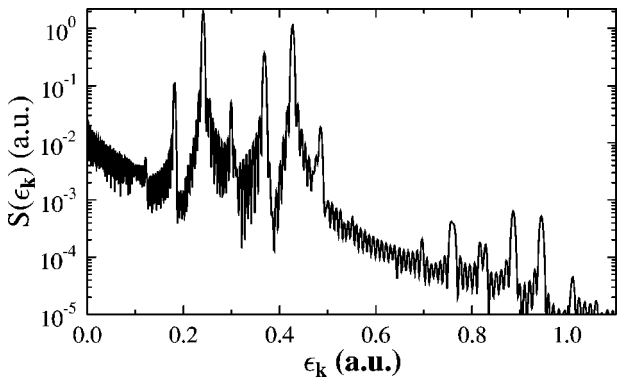

FIG. 13. The photoelectron spectrum for the one-dimensional atom after 128 optical cycles [plus such a fraction of the cycle that $A(t)=0$] for $\xi=0.3$.

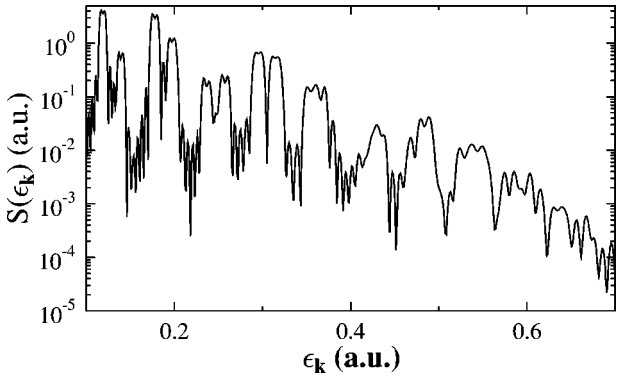

FIG. 14. As in Fig. 13 but for $\xi=1.9$.

our choice of the data the distance between the second and third of those peaks is ω_1. Additional subpeaks are due to the frequency modulation and the distance between each subpeak and the corresponding main peak is again ω_1. The peak at $E_4+\omega$ is significantly heightened due to the presence of the frequency modulation, compared with the case of no modulation (not shown). The pattern is repeated in the second ATI peak (shifted by ω with respect to the first peak, i.e., in the energy range $0.75-1$ a.u.).

In Fig. 14 we show a part of an analogous spectrum for a somewhat stronger frequency modulation ($\xi=1.9$). The structure of the subpeaks is much more complicated because more of the components of the pulse [of amplitudes $J_n(\xi)$] now play important roles. The Rabi frequency corresponding to the nearly resonant coupling of the amplitude $\epsilon_0 J_{-2}(\xi)$ of the states 1 and 2 is now significantly smaller than ω_1. One can thus expect some substructures separated by ω_1, each of them split, with the splitting of the order of twice the Rabi frequency. Such structures are visible in Fig. 14, though the details of the picture are much more complicated.

VI. CONCLUSIONS

We have investigated photoionization and photodetachment of model atomic systems by strong laser pulses with a modulated frequency. We have demonstrated that this may be an important and subtle tool to control the process. We have shown how such a modulation essentially modifies the time evolution of the populations of the discrete states and the photoelectron spectra. The most interesting effects occur for the laser being tuned in the vicinity of the ionization threshold, when the effective detuning during a part of the cycle may be below the threshold, or in the vicinity of the resonant transition between the bound states, when, depending on the modulation depth, the resonance may be either spoiled or restored. Depending on the situation, those effects can be interpreted by introducing the notion of an instantaneous frequency or by considering the electromagnetic field as being composed of photons, which differ in frequency from the optical one by a mutiple of the modulation frequency.

The model developed in the first part of the paper can be used to study the effects of short laser pulses of an arbitrary shape on the dynamics of photodetachment, with the threshold and the continuum-continuum transitions taken into account.

ACKNOWLEDGMENTS

The authors thank Dr. Włodzimierz Jaskólski for providing them with the computer code solving the time-independent Schrödinger equation. This work was supported in part by the Committee for Scientific Research Project No. 2P30207606, and Nicholas Copernicus University Grant No. 380-F. Computations were partially performed at the Interdisciplinary Center for Mathematical and Computational Modelling at the Warsaw University.

[1] *Atoms in Intense Laser Fields*, edited by M. Gavrila (Academic, Boston, 1992).
[2] J. H. Eberly, J. Javanainen, and K. Rzążewski, Phys. Rep. **204**, 331 (1991).
[3] K. Burnett, V. C. Reed, and P. L. Knight, J. Phys. B **26**, 561 (1993).
[4] R. R. Freeman and P. H. Bucksbaum, J. Phys. B **24**, 325 (1991).
[5] H. R. Reiss, Prog. Quantum Electron. **16**, 1 (1992).
[6] H. G. Muller, H. B. van Linden van den Heuvell, and M. J. Van der Wiel, J. Phys. B **19**, L733 (1986).
[7] H. G. Muller, P. Agostini, and G. Petite, in *Atoms in Intense Laser Fields*, edited by M. Gavrila (Academic, Boston, 1992), p. 1.
[8] B. W. Shore, *The Theory of Coherent Atomic Excitation* (Wiley, New York, 1990).
[9] R. R. Jones, Phys. Rev. Lett. **75**, 1491 (1995).
[10] A. Raczyński and J. Zaremba, Phys. Lett. A **232**, 428 (1997).
[11] B. M. Garraway and K.-A. Suominen, Rep. Prog. Phys. **58**, 365 (1995).
[12] P. M. Radmore, S. Tarzi, and K. L. Tang, J. Mod. Opt. **42**, 2213 (1995).
[13] A. Raczyński and J. Zaremba, Phys. Rev. A (to be published).
[14] K. C. Kulander, K. J. Schafer, and J. L. Krause, in *Atoms in Intense Laser Fields*, edited by M. Gavrila (Academic, Boston, 1992), p. 247.
[15] M. Gajda, B. Piraux, and K. Rzążewski, Phys. Rev. A **50**, 2528 (1994).
[16] G. N. Gibson, R. R. Freeman, T. J. McIlrath, and H. G. Muller, Phys. Rev. A **49**, 3870 (1994).
[17] J. H. Eberly, R. Grobe, C. K. Law, and Q. Su, in *Atoms in Intense Laser Fields*, edited by M. Gavrila (Academic, Boston, 1992), p. 301.
[18] K. Rzążewski, L. Wang, and J. W. Haus, Phys. Rev. A **40**, 3453 (1989).
[19] M. Protopapas and P. L. Knight, J. Phys. B **28**, 4459 (1995).
[20] A. Raczyński and J. Zaremba, Phys. Rep. **235**, 1 (1993).
[21] P. W. Milonni and J. R. Ackerhalt, Phys. Rev. A **39**, 1139 (1989).
[22] G. S. Agarwal and W. Harshawardhan, Phys. Rev. A **50**, R4465 (1994).
[23] W. Harshawardhan and G. S. Agarwal, Phys. Rev. A **55**, 2165 (1997).

[24] C. Cohen-Tannoudji, J. Dupont-Roc, and G. Grynberg, *Photons and Atoms — Introduction to Quantum Electrodynamics* (Wiley, New York, 1989).
[25] E. P. Wigner, Phys. Rev. **73**, 1001 (1948).
[26] U. Fano and A. R. P. Rau, *Atomic Collisions and Spectra* (Academic Press, Inc., Orlando, 1986).
[27] A. Raczyński and J. Zaremba, J. Phys. B **29**, 449 (1996).
[28] *Handbook of Mathematical Functions*, edited by M. Abramowitz and J. Stegun (Dover Publications, New York, 1965).
[29] Q. Su and J. H. Eberly, Phys. Rev. A **44**, 5997 (1991).
[30] R. Kosloff, J. Phys. Chem. **92**, 2087 (1988).
[31] P. Bala, P. Grochowski, B. Lesyng, and J. A. McCammon, in *Quantum Mechanical Simulations Methods for Studying Biological Systems*, edited by D. Bicout and M. Field (Springer-Verlag, Berlin, 1996), p. 115.
[32] J. H. Eberly and J. Javanainen, Phys. Rev. Lett. **60**, 1346 (1988).